ELSEVIER

Surface Science 394 (1997) 79–90

surface science

Gas-source growth of group IV semiconductors: I. Si(001) nucleation mechanisms

J.H.G. Owen *, K. Miki, D.R. Bowler, C.M. Goringe, I. Goldfarb, G.A.D. Briggs

Department of Materials, Oxford University, Oxford, OX1 3PH, UK

Received 31 March 1997; accepted for publication 23 June 1997

Abstract

The initial stages of gas-source growth of Si(001) using disilane have been investigated using a combination of elevated-temperature STM and atomistic modelling. The reaction pathway from the initial adsorption of disilane fragments up to the nucleation of short strings of epitaxial dimers is discussed. By the use of our STM to study disilane at the temperatures of interest, and atomistic modelling to calculate structural stability and significant activation barriers, we are able to propose a complete description of the mechanisms which underlie gas-source growth. © 1997 Elsevier Science B.V.

Keywords: Chemical vapour deposition; Density functional calculations; Models of surface chemical reactions; Scanning tunneling microscopy; Silane; Silicon; Single crystal epitaxy; Surface structure

1. Introduction

Due to the dominance of silicon technology in the semiconductor industry, every semiconductor manufacturer would prefer devices based on group IV elemental semiconductors rather than compound semiconductors, if materials with appropriate properties can be produced. In practice, the primary way to tailor the properties is to grow layered silicon/silicon–germanium structures with a spatially varying germanium content. The combined effects of alloying, strain and quantum confinement provide considerable scope for engineering the structural, electronic and optical properties. At relatively low germanium concentrations, for example, graded layers can be made as virtual substrates, while when pure germanium is grown on silicon, quantum dots form spontaneously. Silicon–germanium growth processes are affected by surfactants, which can be used to control roughness and segregation. Hydrogen can be an effective surfactant, so that Ge–Si alloys grown from hydride sources give better controlled changes in composition than materials grown by solid-source MBE.

The scanning tunneling microscope makes it possible to study growth processes in UHV with atomic resolution. Ultimately, one would like to be able to study the growth of Ge–Si alloys. In order to lay a foundation for subsequent studies of Ge–Si growth from hydride sources, it is invaluable first to establish the growth mechanisms of silicon. Although silane (SiH_4) is widely used industrially for reasons of cost, disilane (Si_2H_6) is preferred for laboratory studies because of the

* Corresponding author. Present address: Dept. Chem. Engineering, UCSB, Santa Barbara, CA 93106-5080, USA. Fax: (+1) 805 893.4731; e-mail: jhgowen@squid.ucsb.edu

PII S0039-6028(97)00592-X

lower temperatures at which it decomposes in contact with the substrate [1,2]. In this paper we present studies of nucleation processes by a combination of variable-temperature STM and atomistic modelling. In a companion paper we will present results from in-situ STM movies of the subsequent growth of Si(001) from disilane.

2. Experimental and theoretical methods

Our experiments were performed in a JEOL JSTM-4500XT variable-temperature STM, with a sample stage specified for STM imaging up to 1400 K. In addition to standard UHV facilities, the STM chamber has a gas-handling line for disilane and other hydride sources, with appropriate precautions for safe handling. W tips were prepared by electrochemical etching in 2M KOH. Silicon samples (1.5 mm wide) were cleaved from an n-doped Si(001) wafer, and were prepared with a hydrogen peroxide/sulphuric acid etch before being introduced into UHV and degassed at 700–800 K for several hours. They were then cleaned by repeated flashing to 1400 K for 30 s until the pressure stayed below 10^{-7} Pa during the flash, and then cooled as fast as possible to 900 K to minimise surface reactions. Further cooling to 600 K was performed very slowly, after which no further changes occured.

The measurement of temperature over the ranges of interest presents considerable challenges. A thermocouple gives an accurate measure of the point to which it is attached, but this is not necessarily representative of the surface in the region of interest. Infrared pyrometers operating at wavelengths at which silicon is not transparent are limited in the bottom of their temperature range, and they generally require a larger sample area than we have available. The most accurate method is to use a disappearing filament pyrometer, which can work with very narrow samples. However, this is limited by the temperature range at which visible light is given off to above 1000 K. We therefore developed a calibration curve based on a combination of these techniques and assuming a combination of conduction and radiation losses. This gave an estimated accuracy of ± 30 K, which was undoubtedly the greatest source of uncertainty in our experiments.

The calculations were performed using density functional theory (with the local density approximation) in an implementation called CASTEP [3], and the density matrix method of tight binding [4] in an implementation by Goringe [5]. For the LDA calculations, a slab consisting of five layers of silicon was used, with the bottom layer constrained to lie in bulk-like positions and terminated in hydrogen. Pseudopotentials of the Kerker type, in the Kleinman–Bylander form [6,7] were used, with a cut-off of 115 eV, which is sufficient for energy-difference convergence for the silicon. For the TB calculations, the slab was ten layers thick, with the bottom five layers constrained, and the final layer again terminated in hydrogen. The parameterisation of Bowler et al. [8] was used for the Si–Si and Si–H interactions.

3. Observations

Our experiments build directly on the seminal foundation laid by Bronikowski, Wang and Hamers [1,2], in which Si(001) surfaces were exposed to disilane at room temperature, annealed to a given temperature for a few seconds or longer, and then cooled to room temperature for STM observation. By annealing for gradually longer times or higher temperatures, the sequence of events along the reaction pathway was traced. In their experiments, the various fragments were identified by comparing candidate structures with the observed bonding location of each surface. We have found their interpretation scheme to be consistent, and wherever we have repeated these observations we have come to the same conclusions. Summarising their results, as illustrated in Fig. 1, the disilane gas adsorbs and breaks into SiH_2 and SiH_3 fragments, which break down to adsorbed H and SiH_2 groups over a few minutes at room temperature. These SiH_2 groups react to form first hydrogenated dimers (NRMH) and then clean dimers (SED), which finally diffuse together to

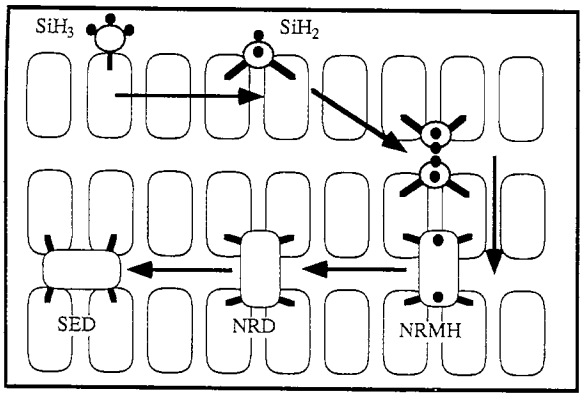

Fig. 1. A schematic of the reaction pathway as described by the Hamers group [1,2]. Initial adsorption is as an SiH_3 group, which adsorbs at one end of a dimer. This decomposes into an SiH_2 group, attached across two dimers, and adsorbed atomic H. Two SiH_2 groups react to form a monohydride ad-dimer adsorbed between two dimer rows. This loses its hydrogen to form a non-rotated clean dimer (NRD), which dissociates into adatoms. These diffuse and form epitaxial dimers (SED) and dimer strings.

form small islands or dimer strings. The major difference between the previous experiments and those described here is that we have performed our experiments and made our observations at elevated temperatures, which has led to new results. In the following sections, we will outline the experimental and theoretical findings for each stage of this rather complex reaction pathway, first summarising previous work, and then detailing our observations. This gives a more logical structure to the paper. At the end, we will then draw together all the results and summarise the complete reaction pathway from the gas phase to small islands as we see it.

3.1. Gas to SiH_2 groups

The products of the dissociative chemisorption of disilane have been identified by Gates [9] using EELS and TPD. Adsorption below 200 K is as an intact molecule into a physisorbed state, but this rapidly breaks up on heating to room temperature, and the majority surface species after room-temperature adsorption are SiH_3, SiH_2 and atomic H. However, a second reaction, via an Si_2H_5 intermediate, has been proposed [10]. This species decomposes, releasing silane (SiH_4) into the gas phase. This mechanism is likely to become more significant at higher H coverages. The SiH_3 groups decompose after a few minutes at room temperature, although the mechanism for this fission is still unknown. In either case, the result of the adsorption reaction is SiH_2 species. No motion of the SiH_2 groups was observed during room-temperature imaging, but there is no correlation between the positions of the fragments at room temperature. The distribution of fragments could be the result of transient mobility during chemisorption or dissociation.

Four different types of feature have been identified, examples of which can be seen in Fig. 2a. The first is a large white dot, placed asymmetrically on the dimer row, but attached to only one dimer. From the identification by the Hamers group, the white dots are SiH_3 groups. The second feature is smaller and is only slightly brighter than the dimers, and is again placed asymmetrically on the dimer row, but has a blackening around it, so that the whole feature is two dimers wide. These are SiH_2 groups bonded in the between-dimer position [11]. Both these features become darker relative to the clean surface at low voltages (Fig. 2b), as would be expected for a hydrogenated species. The hydrogen which results from the decomposition of SiH_3 into SiH_2 can either stick as a single hydrogen atom at one end of a dimer, which will appear bright, or else as two hydrogen atoms on the same dimer, rendering it dark [12]. In the first case, the hydrogen atom will appear quite similar to an SiH_3 group, but becoming brighter at low voltage, whereas an SiH_3 group will become darker. The SiH_3 fragments can be therefore be distinguished from single adsorbed hydrogen atoms. Paired hydrogen atoms can be distinguished from single missing-dimer defects (1-DVs) at low voltage, because the dimers around a 1-DV become bright at low voltages [13]. An example of a defect near a paired hydrogen atom is marked in Fig. 2. The other theoretically stable SiH_2 adsorption site, on top of a dimer without breaking the dimer

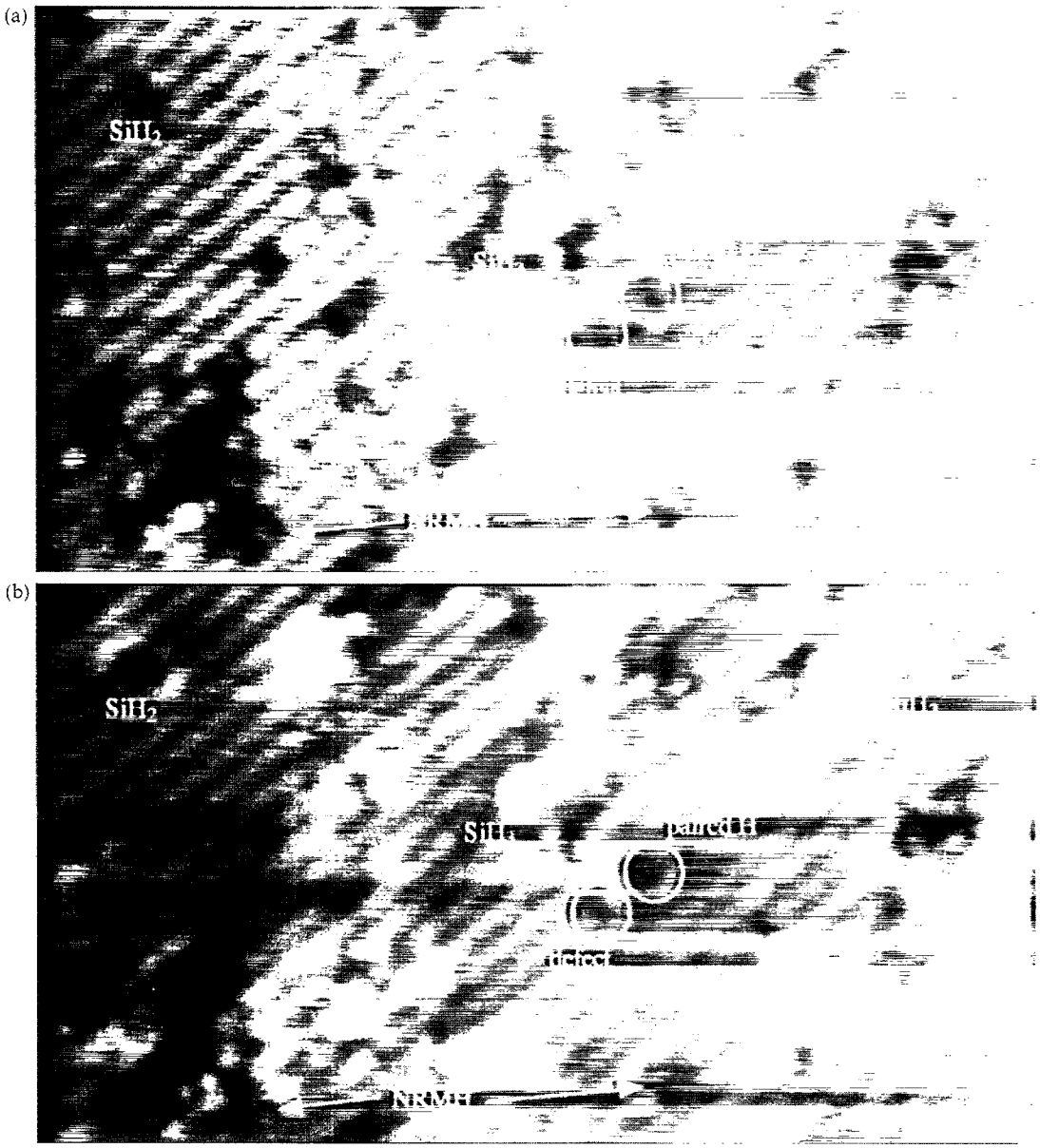

Fig. 2. STM images (28 nm wide) of the Si(001) surface with a small dose of disilane adsorbed at room temperature, taken at a sample bias of (a) −2 V and (b) −1 V. An SiH_3 group, an SiH_2 group, adsorbed hydrogen and a 1-DV defect are marked. The disilane fragments become darker at lower biases, while the 1-DV may be distinguished from the hydrogen-saturated dimer by the enhancement which appears around the defect at low biases.

bond [11], is not seen at low temperatures or coverages, although a few have been seen at higher coverages. The SiH_2 groups seem to be stable at room temperature. By 470 K, they must have become mobile, while remaining intact, as pairs of these groups are seen where there were none before. These groups therefore form the nuclei for the formation of ad-dimers.

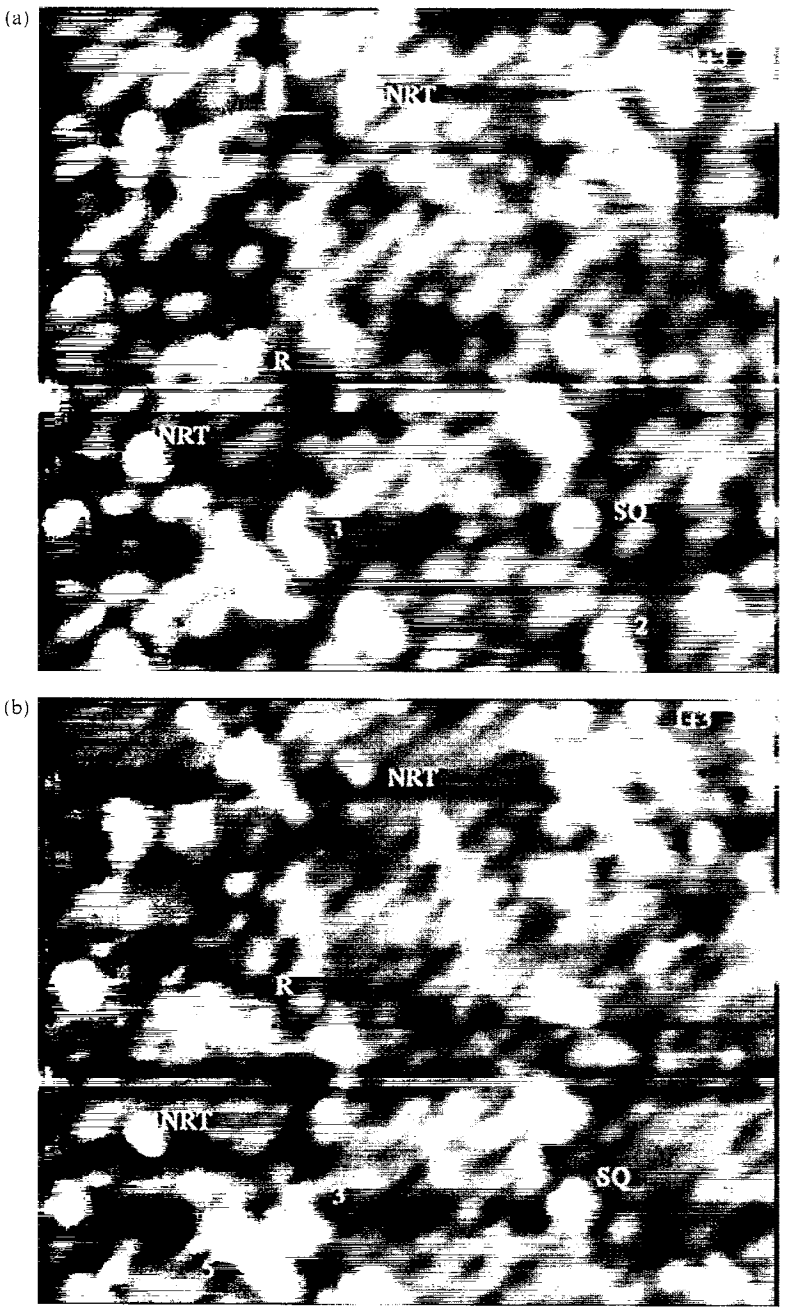

Fig. 3. STM images (15 nm wide) of the Si(001) surface with 0.2 L of disilane adsorbed at 450 K, at a sample bias of (a) −2 V and (b) +2 V. Single epitaxial dimers, in the non-rotated trench position (NRT) and rotated, on-top and trench positions (R, T), diluted dimer strings (2+1), short dimer strings (2, 3, 5) and a square feature (SQ) are marked.

3.2. Formation of monohydride ad-dimer (NRMH) from SiH_2

The primary evidence for this reaction comes from modelling [14], as STM experiments have only seen the precursors and results of the reaction. In our experiments, none of the pairs of SiH_2 groups observed over the course of a few minutes' scanning at 450 K reacted, and above this temperature the disilane reacted on impact to form a mixture of monohydride dimers and clean dimers. The reaction was modelled in LDA, using a unit cell which was two dimer rows wide and two dimers long. Two SiH_2 groups were placed on either side of the trench between dimer rows, and the sole constraint placed on the system was the distance between the two Si atoms. The reaction was modelled by reducing the Si–Si separation in stages, and relaxing the system at each step. There is some significant rearrangement of the groups during the reaction (which is mainly rotation, and therefore energetically cheap), and when the distance between the Si atoms is 2.5 Å, two of the hydrogen atoms spontaneously form H_2(g) and leave the system. The reaction is an irreversible, endothermic reaction, in that the end point is higher in energy than the start point, but as the hydrogen leaves the surface, it is entropically irreversible. The end result is a hydrogenated, non-epitaxial dimer (NRMH) between substrate dimer rows, an example of which can be seen in Fig. 1. The overall barrier for the process is 1.45 ± 0.2 eV, which fits with the observation of these features around 470 K. This dimer structure is the "SiH" group seen in spectroscopy experiments [9].

3.3. Dehydrogenation of a monohydride dimer to form a clean epitaxial dimer

After adsorption at 450 K, some of the disilane fragments have reacted to form clean dimers, and even one or two short dimer strings. The result of dosing the surface under these conditions is shown in Fig. 3, where dimer strings are labelled with a number indicating their length. This means that the NRMH dimers have been able to lose their remaining hydrogen and rotate into the epitaxial direction. The Hamers group observed that the dimers had lost their hydrogen after a 2 min anneal to 470 K, and proposed that the monohydride dimers lose their hydrogen atoms to the substrate slowly, that the non-epitaxial clean dimers dissociate and diffuse as atoms until they can form a dimer in the epitaxial direction. Modelling [15–17] suggests that dimer dissociation and concerted atomic diffusion is the lowest-energy pathway. However, unlike in MBE, we do not see long "diluted dimer rows" [18], and thus the dimer atoms must never become truly independent species. An alternative route from the non-epitaxial direction into the epitaxial direction would be for the dimer to rotate, while remaining intact. The rotation of a dimer on top of a dimer row has been observed [19], and we have observed the rotation of a clean dimer over the trench (which can be seen occurring between the frames of Fig. 4). In all the occurrences that we have found in our STM pictures, the dimers which have been observed rotating have been associated with a defect, and so this rotation probably does not represent a typical situation. The dimer rotates about once every 18 s at 400 K, which gives a barrier of about 1.2 eV, assuming a prefactor of $10^{13}\ s^{-1}$. The vast majority of the epitaxial dimers are clean, which suggests either that hydrogen desorbs more easily from these dimers, or that it is lost somewhere along the reaction pathway between the initial hydrogenated dimers and the epitaxial strings. However, it is not obvious how the dimers are able to lose their hydrogen at 450 K, when the peak desorption temperature for hydrogen from the monohydride phase is 790 K [20]. We propose that these two phenomena are related, and that rotation of ad-dimers, which is a mode not available to the substrate dimers, provides the route for dehydrogenation of the NRMH dimers at such a low temperature. In order to study this, we have performed an LDA calculation of the energy of a clean dimer and a monohydride dimer at different angles between 0° (non-rotated) and 90° (rotated, or epitaxial) [21]. The only constraint upon the system was the angle of the dimer bond about an ⟨001⟩ axis. The result of the calculation is shown in Fig. 5a. A schematic of the structure at significant angles is shown in Fig. 5b. During the process, the dimer has three metastable

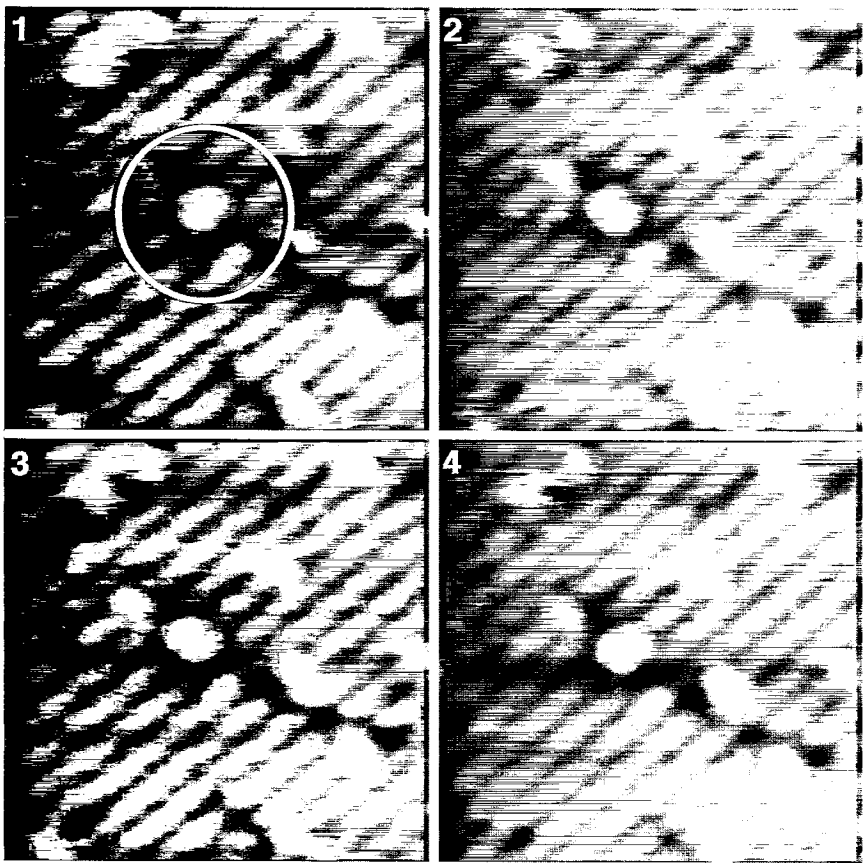

Fig. 4. STM images (12 nm wide) taken at 400 K with a sample bias of +2 V of an rotating ad-dimer in the trench position. Between (1) and (2), the direction of the node in the ad-dimer's π^* orbital has changed by 90°. The speed of rotation corresponds to a barrier of around 1.2 eV, for a pre-exponential factor of 10^{13} s^{-1}.

states: (i) the non-epitaxial position, (ii) a transitional, rotated state, and (iii) the epitaxial position. The barrier to go from the non-epitaxial position to the transitional state is 0.9 eV, while the barrier to go back is 0.2 eV. It can also rotate further from the transitional state, to the epitaxial position, with a barrier of 0.6 eV. To return from the epitaxial direction to the transitional state is a barrier of 0.9 eV. The overall barrier for the complete reaction is around 1.4 eV. The hydrogenated dimer, by contrast, does not form this metastable transitional structure, and the barrier for rotation is about 1.9 eV. Dehydrogenation must therefore occur from a non-rotated dimer, and the ability to rotate may explain the anomalous desorption temperature. We suggest that the dehydrogenation process must be a concerted process involving rotation of the ad-dimer, though we are as yet unsure of the details of the process.

Epitaxial dimers have two bonding sites: either on top of the dimer row (indicated by "R" in Fig. 3), or else between the dimer rows ("NRT" in Fig. 3). The row position is found to be lower in energy than the trench position according to DFT calculations [15,16,22,23]. There is some controversy about this point because STM has found that the majority of dimers sit on top of the rows at 300 K and between the rows at 400 K [24], and empirical modelling has found the between-rows position to be more stable. In a recent paper [25] a reason for this apparent discrepancy has been proposed, involving two

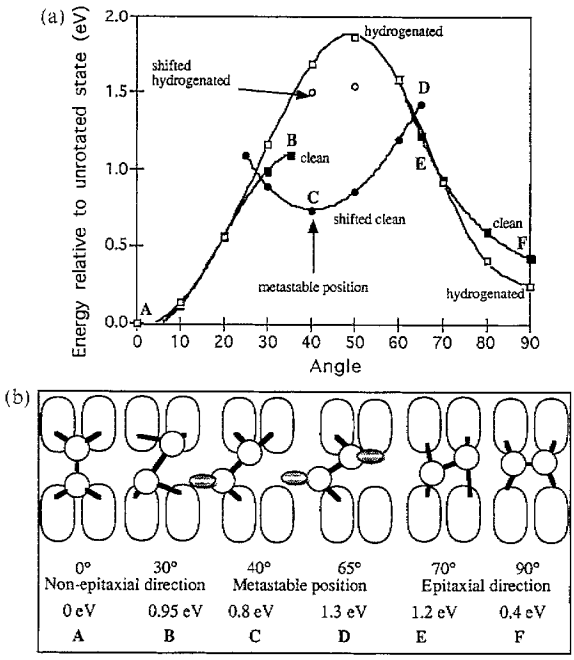

Fig. 5. A graph showing the energy barrier for rotation of clean and hydrogenated dimers in the trench position (a), and a schematic of the structure at significant angles (b). 0° represent the non-rotated position, and 90° the rotated, epitaxial direction. The clean dimer rotates to about 30°, then one of the backbonds breaks and it moves sideways to form a metastable state with a local energy minimum at 40°. This metastable state reverts to the original site at about 60°. The hydrogenated dimer has a much higher barrier to rotation than the clean dimer. In (b), the letters correspond to the positions on the curve in (a). The energy and angle of each structure is also given in (b).

routes for the formation of the dimers, one of which is only accessible at higher temperatures.

3.4. Formation of nucleus structures

The epitaxial dimer is not a stable nucleus for the growth of a new layer since it is a mobile species. The smallest immobile island which we have observed is a dimer string, one dimer wide and three dimers long, with the short edges terminated in the lower-energy rebonded B-type step [26], giving the lowest step-edge energy. The simultaneous conjunction of three mobile dimers to form one of these directly is highly unlikely, and so we must look for a smaller, metastable nucleus which will attract further dimers. There are three major possibilities, which are shown schematically in Fig. 6. First, a pair of dimers both adsorbed on top of the trench, with the dimers in the epitaxial position, which is similar to the MBE "diluted dimer" case [18]. This structure is known as a "T+T". Secondly, two dimers adjacent to each other, one adsorbed over the trench, and the other on top of the dimer row. This is known as a "TR". This is the lowest-energy structure for four silicon atoms on the surface, but is sterically difficult to form. Both of the above structures are seen in our elevated-temperature pictures (Fig. 7). However, we have observed a third structure, which was previously unseen, and is a strong candidate for a nucleus. This structure, the square feature (marked "SQ" in Fig. 3) was not seen by Hamers [1,2], or reported by any of the MBE groups [18,27], though a feature remarkably similar to our structure can be seen in the lower right-hand corner of Fig. 2 in Ref. [18]. Modelling has found that the square can form quite easily from two non-epitax-

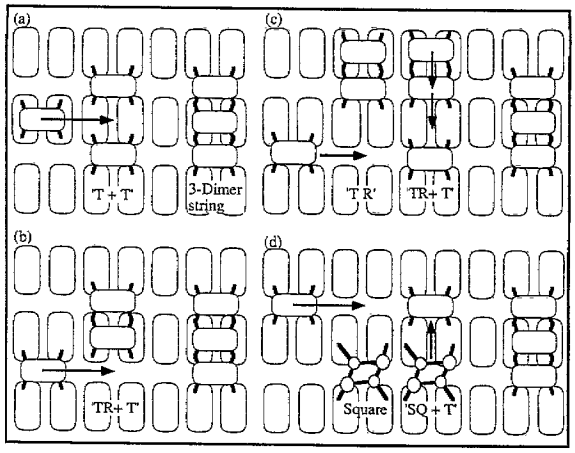

Fig. 6. A schematic diagram of possible nucleation pathways. A pair of trench dimers in neighbouring sites, either rotated or non-rotated, is more stable than independent dimers, and these structures may be immobile long enough for a third row-dimer to fill in the gap and form a length-3 string (a). The non-rotated dimers would have to rotate together, so this may have a higher barrier. The "TR" feature would either have to add a dimer to the "non-sticky" row end (b), or else would require large atom movements to form a string by pinning a dimer at the trench end (c). The favoured pathway is via the square feature (d), where a trench dimer can attach to either end, and then the square would break up into two dimers as a dimer string.

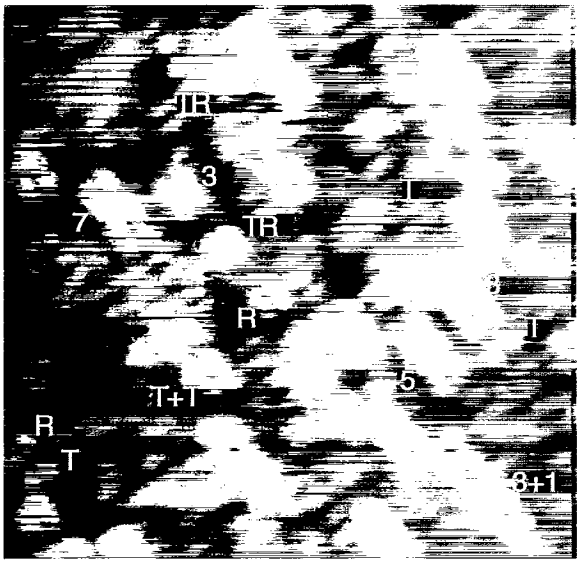

Fig. 7. STM image (16 nm wide) taken at 570 K, with a sample bias of +2 V. The adsorbed disilane has completely reacted to form clean silicon epitaxial dimers. These have all clustered into a variety of short strings. These strings are much shorter than has been observed in MBE at a similar temperature. Some of these strings are labelled. Note that all the ad-dimers are clean.

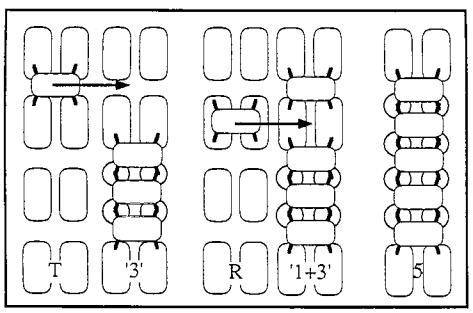

Fig. 8. A schematic picture of the growth process for the dimer strings. The π-bond interaction across dimer rows pins a trench dimer (T) at the site opposite the end of the dimer string (3). This can happen at either end. A diffusing row dimer (R) will then fill in the gap in this "1+3" complex, to form a length-5 string.

ial trench dimers (0.6 eV). A similar though markedly different structure has been seen by Spitzmuller et al. [28] after adsorption of silane and imaging at room temperature. The details of this structure are discussed elsewhere [29], but a ball-and-stick model of the structure calculated from DFT can be seen in Fig. 6d. The initial guess, which was a flat, square ring, spontaneously broke symmetry on being relaxed, to form the rhombohedral structure shown. The four atoms are not in a plane, and so the two higher atoms are shown by larger circles. However, the whole structure can alternate between two different configurations, with the high and low atoms alternating, with a barrier of 0.15 eV, similar to that for a dimer flipping.

Thus the feature seen in the STM pictures would then be an average of these two structures. The square features are seen in our STM pictures at temperatures between 450 and 600 K. They appear during growth before islands are formed, and are the first features seen on top of large epitaxial islands as the second layer begins to nucleate.

The nucleation process going from the three nuclei mentioned above to a string of three dimers has not yet been investigated, but the potential pathways will be described here (see Fig. 6). The "T+T" groups (Fig. 6a) are 0.1 eV lower in energy than two isolated dimers. This interaction energy occurs because the substrate dimer between the ad-dimers is completely saturated, and fewer substrate dimers are affected than when the trench dimers are isolated. This interaction may pin two dimers into a stationary state long enough for a third dimer to join them and create a length-3 string. "Diluted dimer" rows, which have been proposed as a nucleus in MBE [15,16,18], are not seen here. The "TR" feature may be able to add a third ad-dimer, either by adsorbing a trench dimer at the "non-sticky" row end (Fig. 6b), or by pinning a trench dimer at the "sticky" trench end, but this latter requires large atom movements (Fig. 6c). The square feature (Fig. 6d) is 0.3 eV higher in energy than the TR feature [29], but is easy to form and is seen in great profusion during our experiments (Fig. 3). Tight-binding modelling of square and dimer complexes finds that a trench dimer is 0.1 eV lower in energy when it is next to a square than when it is elsewhere. Moreover, a trench dimer could attach at either side of a square, unlike the "TR" structure, so its activity is doubled. Once pinned, the square–trench dimer system can reform into a dimer string of length 3. The barrier for this process is about 1.5 eV [30]. Due to its ease of formation, stability and ease of

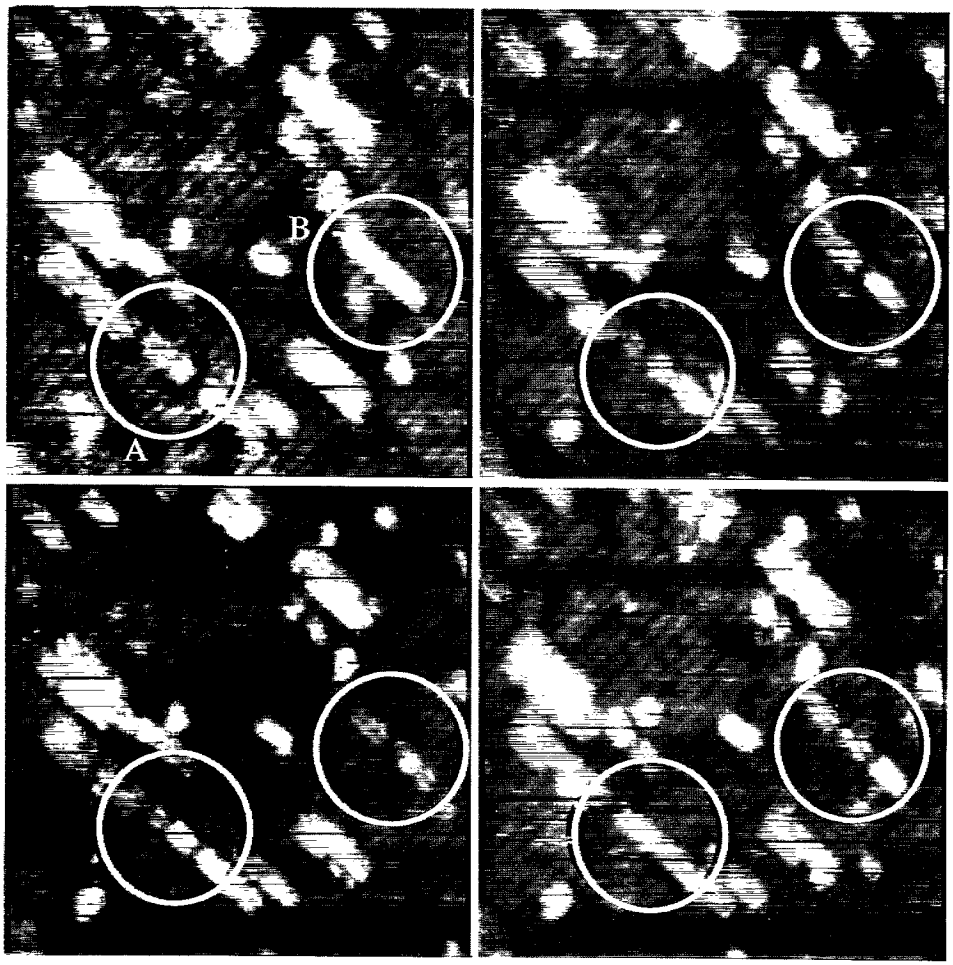

Fig. 9. STM images (20 nm wide) taken at 600 K at a sample bias of +2 V. The four frames are each separated by 18 s. The majority of the dimers on the surface have clustered into groups aligned perpendicular to the underlying dimer rows. These "broken chains" are continuously condensing into complete dimer strings (A) and breaking up again (B).

conversion into a dimer string, we propose the square as the favoured nucleus structure.

3.5. *Addition of dimers onto length-3 string growth*

Once the initial length-3 string has formed, additional dimers can adsorb onto the end. In order to maintain the rebonded structure at the end of the string, these dimers must adsorb in pairs. Studies of step motion [31] and dimer string growth [32] have found that the unit of change is always two dimers, and that the rate of growth is independent of the length of the string. Fig. 7 shows the variety of structures which this process generates on the surface. The addition reaction is shown schematically in Fig. 8. An isolated, mobile dimer is pinned into a trench position opposite the end of the dimer string. This gives a "3+1" structure, as seen in Fig. 7. This structure is then stable until a row dimer fills in the gap, and the string grows by two dimers. This process can be seen occurring on a large scale in Fig. 9. Most of the ad-dimers on the surface have coalesced into chains of dimers, often with gaps in them, but all lined up into broken strings. Isolated dimers are not stationary at this temperature: some streaks

along the dimer rows have been seen, which are likely to be mobile silicon. The gaps in the strings are not fixed, as from picture to picture gaps in one string fill in ("A" in Fig. 9), while in another, a complete string breaks up ("B" in Fig. 9) into smaller units, probably length-3 strings or larger. Thus the step-by-step growth described in Fig. 8 demonstrates the mechanism, but in the real process there are additional interactions between different dimer strings.

4. Conclusions: the reaction pathway from gas to island

To summarise, disilane adsorbs and breaks down to yield SiH_2 groups and hydrogen. From the changing appearance of the surface, we believe that these SiH_2 groups must start to diffuse by 470 K. Two SiH_2 groups on adjacent dimer rows react to form a non-epitaxial hydrogenated ad-dimer between the dimer rows, with a barrier of 1.45 eV. We believe that this dimer is able to lose its hydrogen at this low temperature via a concerted rotation–dehydrogenation mechanism, as this explains the observed facts well. We have observed a square structure, which we believe to be the nucleus for strings of three dimers, which are the shortest strings observed. These strings then grow by addition of pairs of dimers to rebonded, B-type ends, although we have observed these longer strings breaking up as well as growing. A complete reaction pathway as proposed is shown in Fig. 10. How growth proceeds from such dimer strings to complete monolayers will be described in our next paper [33].

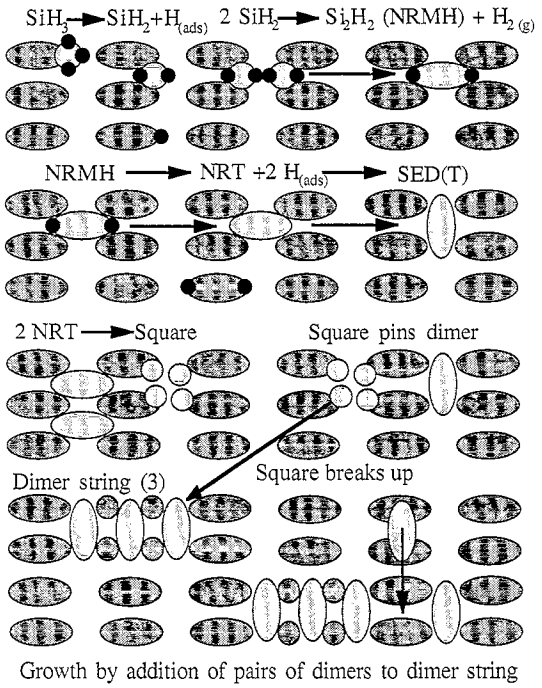

Fig. 10. Our proposed reaction pathway from disilane to dimer string. The disilane breaks up on contact into SiH_2 groups and adsorbed H. Two of the SiH_2 groups react, losing hydrogen to the gas phase, forming a monohydride dimer (NRMH), which loses its hydrogen in a concerted rotation–dehydrogenation mechanism. The clean dimers then rotate into the epitaxial direction, and diffuse to form islands. The nucleus of an island may be the square feature we have observed, formed from a pair of clean non-epitaxial dimers, which attracts a third dimer and may then re-form into a short dimer string. These dimer strings attract further trench dimers, pinning them into place until a row dimer fills in the gap.

Acknowledgements

We would like to thank Henry Weinberg, Martin Castell, David Pettifor and Carl Sofield for useful discussions. J.H.G.O. and D.R.B. are funded by the EPSRC, and J.H.G.O. was partly funded by AEA Technology, Harwell. C.M.G. is a research fellow of Linacre College, Oxford. Computing facilities were provided by the Materials Modelling Laboratory, Oxford (MML), which is partially funded by EPSRC grant GR/H58278.

References

[1] M.J. Bronikowski, Y. Wang, M.T. McEllistreem, D. Chen, R.J. Hamers, Surf. Sci. 298 (1993) 50.
[2] Y. Wang, M.J. Bronikowski, R.J. Hamers, Surf. Sci. 311 (1994) 64.
[3] M.C. Payne, M.P. Teter, D.C. Allan, T.A. Arias, J.D. Joannopoulos, Rev. Mod. Phys. 64 (1992) 1045.
[4] P. Li, R.W. Nunes, D. Vanderbilt, Phys. Rev. B 47 (1993) 10891.
[5] C.M. Goringe, Modell. Simul. Mater. Sci. Eng., submitted for publication.

[6] G. Kerker, J. Phys. C. 13 (1980) 189.
[7] L. Kleinman, D.M. Bylander, Phys. Rev. Lett. 4 (1982) 1425.
[8] D.R. Bowler, M. Fearn, C.M. Goringe, A.P. Horsfield and D.G. Pettifor, J. Phys.: Condens. Matter, submitted for publication.
[9] S.M. Gates, J. Phys. Chem. 96 (1992) 10439.
[10] L.-Q. Xia, M.E. Jones, N. Maity, J.R. Engstrom, J. Chem. Phys. 103 (1995) 1691.
[11] D.R. Bowler, C.M. Goringe, Surf. Sci. 360 (1996) L489.
[12] J.J. Boland, Adv. Phys. 42 (1993) 129.
[13] J.H.G. Owen, D.R. Bowler, C.M. Goringe, K. Miki, G.A.D. Briggs, Phys. Rev. B 54 (1996) 14153.
[14] D.R. Bowler, C.M. Goringe, in preparation.
[15] T. Yamasaki, T. Uda, K. Terakura, Phys. Rev. Lett. 76 (1996) 2949.
[16] K. Terakura, T. Uda, T. Yamasaki, T. Myazaki, Surf. Sci. 357/358 (1996) 394.
[17] C.M. Goringe, D.R. Bowler, Phys. Rev. B, in press.
[18] P.J. Bedrossian, Phys. Rev. Lett. 74 (1995) 3648.
[19] B.S. Swartzentruber, Phys. Rev. Lett. 77 (1996) 2518.
[20] W. Widdra, C. Huang, G.A.D. Briggs, W.H. Weinberg, J. Electron Spectrosc. 6465 (1993) 129.
[21] D.R. Bowler, Ph.D. Thesis, Oxford University, 1997.
[22] G. Brocks, P.J. Kelly, R. Car, Phys. Rev. Lett. 66 (1991) 1729.
[23] G. Brocks, P.J. Kelly, R. Car, Phys. Rev. Lett. 76 (1996) 2362.
[24] Z. Zhang, F. Wu, H.J.W. Zandvliet, B. Poelsema, H. Metiu, M.G. Lagally, Phys. Rev. Lett. 74 (1995) 3644.
[25] A.P. Smith, H. Jonsson, Phys. Rev. Lett. 77 (1996) 1326.
[26] D.J. Chadi, Phys. Rev. Lett. 43 (1979) 43.
[27] A. van Dam, J. van Wingerden, M.J. Haye, P.M.L.O. Scholte, F. Tuinstra, Phys. Rev. B 54 (1996) 1557.
[28] M. Fehrenhacher, J. Spitzmuller, U. Memmert, A.H. Rauscher, M. Pitter, R.J. Behm, J. Vac. Sci. Technol. A 14 (1996) 1499.
[29] J.H.G. Owen, D.R. Bowler, C.M. Goringe, K. Miki, G.A.D. Briggs, Surf. Sci. 382 (1997) L678.
[30] D.R. Bowler, C.M. Goringe, in preparation.
[31] N. Kitamura, B.S. Swartzentruber, M.G. Lagally, M.W. Webb, Phys. Rev. B 48 (1993) 5704.
[32] C. Pearson, M. Krueger, E. Ganz, Phys. Rev. Lett. 76 (1995) 2306.
[33] J.H.G. Owen, K. Miki, D.R. Bowler, C.M. Goringe, I. Goldfarb, G.A.D. Briggs, Surf. Sci, 394, (1997), this issue.